

# Optimal Beam Association for High Mobility mmWave Vehicular Networks: Lightweight Parallel Reinforcement Learning Approach

Nguyen Van Huynh, Diep N. Nguyen, Dinh Thai Hoang, and Eryk Dutkiewicz

## Abstract

In intelligent transportation systems (ITS), vehicles are expected to feature with advanced applications and services which demand ultra-high data rates and low-latency communications. For that, the millimeter wave (mmWave) communication has been emerging as a very promising solution. However, incorporating the mmWave into ITS is particularly challenging due to the high mobility of vehicles and the inherent sensitivity of mmWave beams to the dynamic blockages, resulting in frequent handover and higher latency/disconnection time. Thus, this article develops an optimal beam association framework for the mmWave vehicular networks under high mobility. Specifically, we use the semi-Markov decision process (SMDP) to capture the dynamics and uncertainty of the environment. The Q-learning algorithm is then often used to find the optimal policy. However, Q-learning is notorious for its slow-convergence. Hence, we leverage the fact that there are usually multiple vehicles on the road to speed up the convergence to the optimal solution. To that end, we develop a lightweight yet very effective parallel Q-learning algorithm to quickly obtain the optimal policy by simultaneously learning from various vehicles. Extensive simulations demonstrate that our proposed solution can increase the data rate by 60% and reduce the disconnection time by 33% compared to other solutions.

## Index Terms

millimeter wave, vehicular networks, high mobility, handover, beam selection, parallel Q-learning.

Nguyen Van Huynh, Diep N. Nguyen, Dinh Thai Hoang, and Eryk Dutkiewicz are with University of Technology Sydney, Australia.

E-mails: huynh.nguyenvan@student.uts.edu.au, {Diep.Nguyen, Hoang.Dinh, and Eryk.Dutkiewicz}@uts.edu.au.

## I. INTRODUCTION

Over the past few years, the explosive growth of interest in intelligent transportation and vehicular communications offers a great potential to enhance traffic efficiency, improve road safety, and enable open disruptive entertainment services and autonomous driving [1], [2]. These applications often require low-latency, high reliability, and especially multi-Gbps network access. For instance, Google's self-driving car in a second can generate up to 750 MB of data [3]. It is expected that a vehicle may produce 1 Terabyte of data in a single trip [1]. To address this critical problem, the emerging millimeter wave (mmWave) communication has been recently considered as a very promising solution [4]. Comparing with existing wireless networks, the mmWave technology operates at much higher carrier frequencies, i.e., from 30 GHz to 300 GHz. Thus, it possesses much more abundant spectrum resources, resulting in potentially extremely high data rates and low-latency communications. Nevertheless, in mmWave communications, the temporal degradation of channel quality occurs much more frequently than conventional (lower frequency) communications due to high propagation attenuation, selective directivity, and severe susceptibility to blockages, especially in vehicular communications under high mobility. This work aims to address these problem to enable mmWave communications under high mobility.

### A. *Related Work and Motivation*

Several studies in the literature have been proposed to address the above inherent limitations of mmWave communications [5]-[12]. In [5], the authors proposed a novel scheduling framework to schedule communication tasks on both conventional microwave and mmWave bands. Similarly, in [6], the authors introduced a new protocol that enables simultaneously connections to conventional 4G cells and 5G mmWave cells. In [8], the authors considered the throughput maximization problem in mmWave ultradense networks using dynamic spectrum sharing.

Although the aforementioned solutions and others in the literature can improve the performance of mmWave systems, they did not account for the high mobility of vehicles and dynamics of the environment, hence are inapplicable to such a scenario. In [13], the authors pointed out that one challenge when incorporating mmWave into vehicular networks is that mmWave must support ultra-fast data exchanges between infrastructure (e.g., road side units (RSUs)) and vehicles. Thus, the authors proposed an adaptive channel

estimation mechanism for beamforming with the aid of location information to solve the problem. The position information is then demonstrated as an important factor to greatly improve the initial association of vehicles to the infrastructure. Similarly, in [14], the authors introduced a beam switching mechanism in mmWave vehicle-to-infrastructure communications. Differently, the authors in [15] studied the transmission range of mmWave microcellular networks in urban areas with vehicle-to-infrastructure communications using stochastic geometry. In particular, the authors first derived the coverage probability under certain base station association conditions and then obtained closed-form policies. The authors showed that non-line-of-sight base stations have little impact on the association process, and they are not the source of interference in almost scenarios.

It is important to note that these works and many others in the literature cannot deal with the dynamic and uncertainty of the system in which the channel quality is usually degraded due to the intermittent connectivity of mmWave links. For that, in [16], the authors proposed an online learning algorithm to obtain the optimal beam selection policy based on the prior environment information. This problem is first modeled as a contextual multi-armed bandit problem. Then, the learning algorithm is developed to guide the mmWave base station to select an optimal subset of beams for vehicles by exploiting coarse user location information. The simulation results confirmed the efficiency of the proposed solution. Nevertheless, in this paper, the authors only attempted to obtain the optimal beam selection for a single base station. In practice, multiple base stations are often in place, and they can cooperate to achieve a globally optimal beam selection solution. In addition, the high mobility of vehicles has not been studied. In [17], the authors considered the vehicle-cell association problem for mmWave vehicular networks to maximize the average rate of vehicles. Specifically, the authors first formulated the problem as a discrete non-convex optimization problem. Then, a learning algorithm is developed to estimate the solution for the non-convex optimization problem. Although achieving a good data rate and low signaling overhead, the effects of the high mobility and blockage on beam association/handover have not been considered.

Given the above, this work aims to develop an optimal beam association framework for mmWave vehicular communications under the high mobility of vehicles and the uncertainty of blockages. We adopt the data rate, handover overhead, and disconnection time as major performance metrics. In particular, to capture the dynamics of blockages, channel quality, and mobility, we first model the problem as

a semi-Markov decision process (SMDP). The Q-learning algorithm is then often adopted to solve the optimization problem the underlying SMDP. Nevertheless, the Q-learning algorithm is well known for its slow convergence rate, especially in dynamic and complicated environments. Instead of adopting deep reinforcement learning structures e.g., double deep Q-learning, deep dueling (like most works in the literature, e.g., [17]), in this article, we leverage the fact that there are usually multiple vehicles on the road to speed up the convergence to the optimal solution. To that end, we develop a lightweight yet very effective parallel Q-learning algorithm to quickly obtain the optimal policy by simultaneously learning from various vehicles. Specifically, vehicles on the road can act as active learners to help the system simultaneously collect data. Based on the collected data, the proposed parallel Q-learning algorithm can *quickly learn* the environment information, e.g., RSSI profile, beam's location, vehicle's velocity, and blockage, to derive the optimal beam association strategy. The proposed parallel Q-learning algorithm does not only require lower complexity but also converge faster than the latest deep learning-based approaches (e.g., double Q-learning, deep dueling). Moreover, unlike deep reinforcement learning methods (e.g., [17]), our proposed parallel Q-learning framework is proven to always converge to the optimal policy. We show that the high mobility and parallelism of vehicles now become helpful in speeding up the learning process of our underlying algorithm.

It is worth noting that unlike existing works, e.g., [16], [17], in which learning algorithms are deployed at the vehicles with limited resources, in our design, the eNodeB executes the parallel Q-learning algorithm and sends optimal beam association/handover actions to vehicles. As such, the computing complexity is moved to the eNodeB. The simulation results then show that our proposed parallel Q-learning algorithm can increase the data rate for each vehicle by up to 60% and reduce the disconnection time by 33% compared to existing approaches.

## B. Main Contributions

In the following, we highlight the key contributions of this paper.

- Develop an optimal beam association solution for mmWave vehicular communication networks using the semi-Markov decision process framework to capture the dynamics and uncertainty of the environment, e.g., beam's location, RSSI profile, the velocity of the vehicle, blockages.

- Develop a lightweight yet very effective parallel Q-learning algorithm to quickly obtain the optimal policy by leveraging simultaneous learning from various vehicles. The proposed parallel Q-learning algorithm does not only require lower complexity but also converge faster than latest deep learning-based approaches. Specifically, the algorithm deploys multiple learning processes at the eNodeB, and each learning process is assigned to learn from a vehicle on the considered road to update the global policy.
- Prove that the proposed parallel Q-learning framework converges with probability one to the optimal policy. Note that deep Q-learning based approaches are not always guaranteed to converge. We also provide comprehensive analysis on the convergence time/rate, complexity, and overhead of the proposed framework.
- Perform extensive simulations to demonstrate the effectiveness of the proposed parallel Q-learning algorithm. By learning from multiple vehicles and exploit the high mobility of vehicles, our proposed algorithm can achieve the performance close to that of the hypothetical scheme which requires complete environment information in advance.

The rest of paper is organized as follows. The system model is described in Section II. In Section III, we present the problem formulation based on the SMDP. Then, Section IV describes the conventional Q-learning algorithm and our proposed parallel Q-learning algorithm. After that, we provide the evaluation results in Section V. Finally, the conclusion is highlighted in Section VI.

## II. SYSTEM MODEL

Consider a millimeter wave (mmWave) vehicular network, where an LTE eNodeB and a set of  $N$  mmWave base stations (mmBSs)  $BS = \{BS_1, \dots, BS_n, \dots, BS_N\}$  are deployed as shown in Fig. 1. This is an expected network model for 5G and beyond systems [18]-[20]. All the mmBSs can connect to the eNodeB via backhaul links. Each vehicle is equipped with two communication interfaces: (i) an LTE interface to communicate with the eNodeB and (ii) an mmWave interface to communicate with an mmBS [16]. The Friis free-space equation reveals that with given transmit power and antenna gains, the pathloss increases when the frequency increases [1], [34]. For example, increasing the carrier frequency

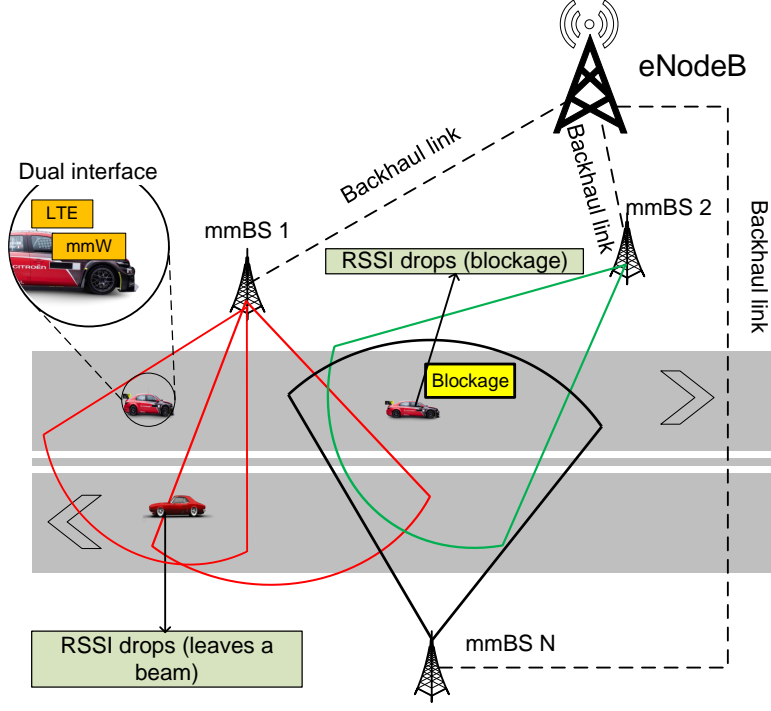


Fig. 1: System model

from 2 GHz to 60 GHz<sup>1</sup> results in an increase of 29 dB for the pathloss. The mmWave signals also suffer from obstacles and scattering objects (both static and dynamic). Thus, the path loss model between the vehicle and the mmBS can be formulated as follows [1], [34]:

$$PL(d)[dB] = PL(d_0) + 10n \log_{10} \frac{d}{d_0} + \psi = 20 \log_{10} \frac{4\pi d_0}{\lambda} + 10n \log_{10} \frac{d}{d_0} + \psi, \quad (1)$$

where  $d_0$  is the reference distance,  $PL(d_0)$  is the free-space loss at the reference distance,  $n$  is the path loss exponent,  $d$  is the distance between the vehicle and the mmBS,  $\lambda$  is the carrier wavelength, and  $\psi$  is the log-normal *shadowing loss* caused by the absorption of obstacles and scattering objects. Moreover, the log-normal *shadowing loss* increases with distance between the vehicle and the mmBS as the farther the transmitter and the receiver are the more likely that there are obstructing objects in between them. When the path loss increases, the received power at the mmBS decreases. Thus, when the vehicle leaves a beam or moves to a blockage zone, the received signal strength indicator (RSSI) will drop. As such, the vehicle is

<sup>1</sup>60 GHz is the common frequency band used for automotive communications.

not be able to communicate with its connected mmBS (through the beam). To avoid disrupting the service, the vehicle needs to connect to another beam which provides better channel quality. This beam can belong to the current connected mmBS, i.e., beam association, or belong to another mmBS, i.e., handover.

Conventional methods in the literature [26]-[28] usually make a beam association/handover decision based on the current channel information or network state, e.g., SINR or RSSI, where the decision is triggered when the SINR/RSSI are dropped due to blockage objects or mobility. However, these solutions may lead to too frequent handover and hence the associated handover cost/interruption, especially in mmWave networks where the temporal degradation of channel quality frequently occurs due to the intermittent connectivity of mmWave links. In addition, as the mmWave communication quality often deteriorates intermittently and rapidly, these solutions may lead to the ping-pong effect resulting in high outage probability and low system performance [29], [30].

In this paper, our learning algorithm can efficiently address these critical problems by learning the environment conditions. In particular, we consider a centralized controller, i.e., the eNodeB, that “learns” from vehicles on the considered road and makes beam association/handover decisions for all vehicles. With the proposed learning algorithm, the eNodeB can learn the RSSI profiles of the beams in the systems. To reduce the number of beam association/handovers, the eNodeB can guide the vehicle to connect to a beam with a “better” RSSI profile (in terms of the long-run average data rate). In addition, the beam association/handover decision can be triggered even when the RSSI level is still good to anticipate the intermittent problem of mmWave links. It is worth noting that the RSSI level can be inferred by the mmBS through the received signals from the vehicle. Moreover, with current standards in ITS systems [35], the mmBS always has the location of its connected vehicles. Based on this information, the eNodeB runs the algorithm to obtain the best beam for the vehicle to connect without adding noticeable overhead to current ITS systems.

We assume that each mmBS  $BS_n$  has a finite set  $\mathcal{B}_n = \{b_{n,1}, \dots, b_{n,k}, \dots, b_{n,K}\}$  of  $K$  orthogonal beams [16]. Based on the information learned from the vehicle, i.e., location, velocity, and RSSI level, the eNodeB selects beam  $b_{n,k}$  of mmBS  $BS_n$  to support the communications of the vehicle. In this paper, the velocity of each vehicle is not fixed and follows the Gaussian distribution. When the vehicle is connected to beam  $b_{n,k}$ , it can successfully transmit data with rate  $r_{n,k}$ . Note that  $r_{n,k}$  is a random variable, depending

on the RSSI level (i.e., channel quality) of the channel. Consider  $M$  RSSI levels  $\mathcal{R} = \{0, 1, \dots, M-1\}$  which depend on the environmental conditions, e.g., channel conditions (as modeled above) and blockage probability. The higher the RSSI level is, the higher the achievable data rate of the vehicle. We assume that when the vehicle enters blockage zone, the RSSI level drops to 0, and thus the vehicle cannot connect to the mmBS. We then define  $\omega_{b_n^k}$  is the blockage probability of beam  $b_{n,k}$  with  $0 \leq \omega_{b_n^k} \leq 1$ .  $\omega_{b_n^k} = 1$  if there are static blockage objects (e.g., buildings) in the coverage of the beam. Similar to [16], we assume that  $r_{n,k}$  is varied from 0 to  $R_{\max}$ , where  $R_{\max}$  is the maximum achievable rate, corresponding to the highest RSSI level. Formally,  $r_{n,k}$  can be formulated as in (2).

$$r_{n,k} = \begin{cases} 0, & \text{with probability } \omega_{b_n^k}, \\ \Delta(l), l \in \{\mathcal{R} \setminus \{0\}\}, & \text{with probability } 1 - \omega_{b_n^k}, \end{cases} \quad (2)$$

where  $\Delta(l)$  is the rate corresponding to the current RSSI level  $l$  [16]. Note that to capture the fading effect of the channel,  $\Delta(l)$  follows a given random distribution.

Note that although the above environment information (e.g., the RSSI profiles, vehicle velocities, and the blockage probability) are required for the modeling/formulation purpose, the proposed parallel Q-learning algorithm below does not require these parameters explicitly as input. Instead, after executing an action, the eNodeB observes the *reward*, i.e., the actual data rate between the vehicle and the connected mmBS. The reward function (defined below) hence captures the communication channel between vehicles and mmBSs (e.g., the bit error rate and fading). The details of the proposed algorithm are described in the next section.

### III. PROBLEM FORMULATION

As mentioned, in this work, we aim to deal with the dynamics of blockages, channel quality, and mobility. However, the conventional Markov decision process is not effective in capturing the dynamics and uncertainty of the system. Thus, in this work, we propose to use the semi Markov decision process (SMDP) [21]. Different from the MDP, in an SMDP, an action is only taken when an event occurs, i.e., decision epoch. An SMDP can be defined as a tuple  $\langle t_j, \mathcal{S}, \mathcal{A}, r \rangle$ , where  $\mathcal{S}$  and  $\mathcal{A}$  are the state space and the action space of the system, respectively.  $t_j$  defines decision epoch  $j$ -th when an event occurs, and  $r$  is the reward function.



### A. State Space

The system's state space is represented as the discretized space of RSSI levels and the connected beam of the current vehicle. Thus, the system's state space  $\mathcal{S}$  is defined as follows:

$$\mathcal{S} \triangleq \left\{ (l, b_{n,k}) : l \in \{0, \dots, m, \dots, M-1\}, b_{n,k} \in \mathcal{B}_n \cup \{b_{0,0}\}, \right. \\ \left. \forall n \in \{1, \dots, N\}, \forall k \in \{1, \dots, K\} \right\}, \quad (3)$$

where  $l$  is the RSSI level of the current vehicle and  $b_{n,k}$  is the current connected beam of the current vehicle.  $b_{0,0}$  is a virtual beam used to capture the case that there is no available beam at a given location of the current vehicle. In this case, the RSSI level of the current vehicle is always 0. Note that we choose not to have the vehicle's velocity as part of the system stage. Instead, the vehicle's velocity is implicitly captured through the actual average data rate, i.e., reward, when an action is made (as discussed in the Section III-C). The effects of the vehicle's velocity on the system performance as well as the convergence time of the algorithm will be also comprehensively discussed in the simulation results.

The road is modeled as an one-dimension area  $\mathcal{W} \in \mathbb{R}$  that is discretized to  $\lfloor \frac{W}{z} \rfloor$  zones, where  $W$  is the length of the considered road,  $z$  is the length of each zone, and  $\lfloor \cdot \rfloor : \mathbb{R} \rightarrow \mathbb{N}$  is the floor function. When the vehicle at location  $w \in \mathcal{W}$ , the vehicle is at zone  $\lfloor \frac{w}{z} \rfloor$ -th. At the current state  $s \in \mathcal{S}$ , an event  $e_s$  is triggered if a vehicle reaches a new zone. Note that as the vehicle's speed is not fixed, the time interval between two consecutive epochs varies. To capture that, the semi-Markov decision process is used in this work, instead of the conventional Markov decision process with identical time slots.

### B. Action Space

When the vehicle reaches a new zone on the road, i.e., event  $e_s$  is triggered (given its current state  $s \in \mathcal{S}$ ), the eNodeB decides if the vehicle needs to associate to a new beam or stay on the current beam. The action space  $\mathcal{A}_s$  of the system is then defined as follows:

$$\mathcal{A}_s \triangleq \{a\} = \{b_{n,k}, b_{0,0}\}, \forall n, \forall k, \quad (4)$$

where  $a$  is the action made at state  $s$ .  $a = b_{n,k}$  if the eNodeB guides the vehicle to connect to beam  $b_{n,k}$ , i.e., beam  $k$ -th of mmBS  $BS_n$ . This includes the case staying with the current beam.  $a = b_{0,0}$  if there is no available beam at the current location.

### C. Immediate Reward

In this paper, we aim to maximize the long-term average data rate of the system. As mentioned, at decision epoch  $t$ , if an action is taken so that the vehicle connects to beam  $b_{n,k}$ , it can communicate with a rate of  $0 \leq r_{n,k} \leq R_{max}$  corresponding to the current RSSI level (from its current state  $s$  defined above).

The resulting data that the vehicle receives from the mmBS is calculated as  $j_{n,k}^t r_{n,k}$ , where  $j_{n,k}^t$  is the connection time between two consecutive decision epochs (during which the vehicle can communicate with the mmBS through beam  $b_{n,k}$ ). As the algorithm observes the reward at the end of each decision epoch,  $j_{n,k}^t$  is the duration from the time that the vehicle enters the current zone until it leaves (the current zone) to enter the next zone.  $j_{n,k}^t$  hence depends on the velocity of the vehicle  $v_t$  at the epoch  $t$ . Practically, the velocity  $v_t$  can change from one to another epoch or even during the time  $j_{n,k}^t$ . However, without loss of generality, we assume that the time  $j_{n,k}^t$  between two consecutive epochs is small enough (e.g., by setting the length per zone  $z$  as small as necessary) so that the vehicle's RSSI level and velocity remain unchanged. Thus, connection time  $j_{n,k}^t$  can be calculated as  $\frac{z}{v_t}$ .

In addition, the service may be interrupted during the handover/beam-switching, denoted as  $h$ , i.e., the time it takes for the vehicle to switch to the new beam. We assume that the handover time is the same for all the beams/mmBSs. Taking the handover time into account, at state  $s \in \mathcal{S}$ , the immediate data rate after performing action  $a$  is obtained in (5).

$$r(s_t, a_t) = \begin{cases} (j_{n,k}^t - h)r_{n,k}, & \text{if } a_t = b_{n,k}, \\ 0, & \text{otherwise,} \end{cases} \quad (5)$$

where  $s_t$  and  $a_t$  are the system state and the action taken at decision epoch  $t$ , respectively and  $r_{n,k}$  is the communication rate when the vehicle connects to beam  $b_{n,k}$  as defined in (2). Clearly,  $j_{n,k}^t$ ,  $r_{n,k}$ , and  $h$  depend on the environment conditions, e.g., blockage, beam's location, RSSI profiles, and the velocity of the vehicle. Our proposed algorithm in the sequel aims to learn these dynamics and uncertainty by interacting with the environment.

### D. Optimization Formulation

The decision policy  $\pi$  of the proposed SMDP can be defined as a mapping from the state space to the action space:  $\mathcal{S} \rightarrow \mathcal{A}_s$  [36], [21]. Thus, with initial state  $s$ , the long-term average data rate is formulated

as follows:

$$\mathcal{R}_\pi(s) = \lim_{T \rightarrow \infty} \frac{\mathbb{E}\{\sum_{t=0}^T r(s_t, \pi(s_t)) | s_0 = s\}}{\mathbb{E}\{\sum_{t=0}^T \xi_t | s_0 = s\}}, \forall s \in \mathcal{S}, \quad (6)$$

where  $\xi_t$  is the time interval between the  $t$ -th and  $(t+1)$ -th decision epochs,  $\pi(s)$  is the action at state  $s$  based on policy  $\pi$ , and  $r$  is the immediate reward after performing an action. In Theorem 1, we will prove that the limit in (6) exists [22].

**THEOREM 1.** *With the number of events in a given time and the number of states in the state space  $\mathcal{S}$  are finite, we have:*

$$\mathcal{R}_\pi(s) = \lim_{T \rightarrow \infty} \frac{\mathbb{E}\{\sum_{t=0}^T r(s_t, \pi(s_t)) | s_0 = s\}}{\mathbb{E}\{\sum_{t=0}^T \xi_t | s_0 = s\}} = \frac{\bar{\mathcal{L}}_\pi r(s, \pi(s))}{\bar{\mathcal{L}}_\pi y(s, \pi(s))}, \forall s \in \mathcal{S}, \quad (7)$$

where  $y(s, \pi(s))$  denotes the expected time interval between two consecutive decision epochs when an action is taken at state  $s$  following policy  $\pi$ .  $\bar{\mathcal{L}}_\pi$  is the limiting matrix of the transition probability matrix  $\mathcal{L}_\pi$  given policy  $\pi$  [21] as defined in the following.

$$\bar{\mathcal{L}}_\pi = \lim_{T \rightarrow \infty} \frac{1}{T} \sum_{t=0}^{T-1} \mathcal{L}_\pi^t, \quad (8)$$

*Proof:* First, we prove the following lemma.

**Lemma 1.** *The limiting matrix  $\bar{\mathcal{L}}_\pi$  of the the transition probability matrix  $\mathcal{L}_\pi$  always exists.*

*Proof:* The proof of Lemma 1 is provided in Appendix A. ■

As the limiting matrix  $\bar{\mathcal{L}}_\pi$  exists (see Lemma 1) and the total probabilities of transiting from a given state to other states equals to 1, i.e.,  $\sum_{s' \in \mathcal{S}} \bar{\mathcal{L}}_\pi(s'|s) = 1$ , we have:

$$\begin{aligned} \bar{\mathcal{L}}_\pi r(s, \pi(s)) &= \lim_{T \rightarrow \infty} \frac{1}{T+1} \mathbb{E}\left\{\sum_{t=0}^T r(s_t, \pi(s_t))\right\}, \forall s \in \mathcal{S}, \\ \bar{\mathcal{L}}_\pi y(s, \pi(s)) &= \lim_{T \rightarrow \infty} \frac{1}{T+1} \mathbb{E}\left\{\sum_{t=0}^T \xi_t\right\}, \forall s \in \mathcal{S}. \end{aligned} \quad (9)$$

Clearly, the long-term average reward in (7) is obtained by taking the ratio of  $\bar{\mathcal{L}}_\pi r(s, \pi(s))$  and  $\bar{\mathcal{L}}_\pi y(s, \pi(s))$ . In addition, the ratio of limits equals to the limit of the ratio. As a result, the long-term average reward in (7) is well defined and exists. ■

Next, in Theorem 2, we prove that the underlying Markov chain is irreducible, and thus the long-term average data rate  $\mathcal{R}(\pi)$  does not depend on the initial state  $s_0$ .

**THEOREM 2.** *For every  $\pi$ , the long-term average data rate  $\mathcal{R}(\pi)$  is well defined and does not depend on the initial state, i.e.,  $\mathcal{R}_\pi(s) = \mathcal{R}_\pi, \forall s \in \mathcal{S}$ .*

*Proof:* The proof of Theorem 2 is provided in Appendix B. ■

Then, the long-term average data rate optimization problem can be formulated as follows:

$$\begin{aligned} \max_{\pi} \quad & \mathcal{R}_\pi = \frac{\overline{\mathcal{L}_\pi r}(s, \pi(s))}{\overline{\mathcal{L}_\pi y}(s, \pi(s))} \\ \text{s.t.} \quad & \sum_{s' \in \mathcal{S}} \overline{\mathcal{L}_\pi}(s'|s) = 1, \forall s \in \mathcal{S}. \end{aligned} \tag{10}$$

Our aim in this work is finding the optimal beam association policy to maximize the long-term average data rate, i.e.,

$$\pi^* = \operatorname{argmax}_{\pi} \mathcal{R}_\pi. \tag{11}$$

#### IV. PARALLEL REINFORCEMENT LEARNING FOR BEAM ASSOCIATION IN HIGH MOBILITY MMWAVE VEHICULAR NETWORKS

In this section, we develop the parallel Q-learning algorithm that obtains the optimal beam association policy much faster than those of the existing reinforcement learning based algorithms (e.g., [17]). For that, we first briefly present the details of the conventional Q-learning algorithm. Related mmWave works in the literature usually adopt the Q-learning and deep Q-learning algorithms to solve their problems. However, with dynamic and complicated system, the Q-learning algorithm usually takes a very long time to obtain the optimal strategy. In addition, the deep Q-learning algorithm (e.g., [17]) requires high performance computing resources and does not always ensure to converge to the optimal policy due to the overestimation of the optimizer.

##### A. Q-Learning Approach

This section presents the Q-learning algorithm [25], which enable the eNodeB to obtain the optimal beam association strategy for vehicles without prior environment parameters, e.g., RSSI profiles and blockages.

The key idea of the Q-learning algorithm is updating the Q-value function for all state-action pairs stored in a Q-table. At a given system state, the Q-learning algorithm performs an action and observes the immediate reward as well as the next state of the system. Based on these observations, the algorithm can update the Q-value for the current state-action pair based on the Q-value function [25]. As such, the learning process is able to learn from the previous experiences, i.e., current state, action, next state, and immediate reward, to derive the optimal solution [25]. In the following, we presents the fundamentals of the Q-value function.

We first define the beam association policy as  $\pi : \mathcal{S} \rightarrow \mathcal{A}$ . In particular,  $\pi$  is a mapping from a given state to its corresponding action. Our aim in this paper is finding the optimal beam association policy  $\pi^*$  to optimize the system performance in terms of the average data rate, disconnection time, and number of handovers. Then, we define  $\mathcal{V}^\pi(s) : \mathcal{S} \rightarrow \mathbb{R}$  as the expected value function of state  $s \in \mathcal{S}$  given policy  $\pi$ .  $\mathcal{V}^\pi(s)$  can be formulated as follows:

$$\mathcal{V}^\pi(s) = \mathbb{E}_\pi \left[ \sum_{t=0}^{\infty} \gamma r_t(s_t, a_t) | s_0 = s \right] = \mathbb{E}_\pi \left[ r_t(s_t, a_t) + \gamma \mathcal{V}^\pi(s_{t+1}) | s_0 = s \right], \quad (12)$$

where  $0 \leq \gamma < 1$  denotes the discount factor. In particular,  $\gamma$  represents the effect of the future rewards. The higher the discount factor is, the more important future rewards are. At each state  $s$ , we aim to find the optimal action to derive the optimal beam association policy  $\pi^*$ , which is a map from a given state to the optimal action. To do that, the optimal value function for each state has to be obtained as formulated in the following:

$$\mathcal{V}^*(s) = \max_a \left\{ \mathbb{E}_\pi [r_t(s_t, a_t) + \gamma \mathcal{V}^\pi(s_{t+1})] \right\}, \quad \forall s \in \mathcal{S}. \quad (13)$$

We then denote the optimal Q-function state-action pair  $(s, a), \forall s \in \mathcal{S}, \forall a \in \mathcal{A}$  as follows:

$$\mathcal{Q}^*(s, a) \triangleq r_t(s_t, a_t) + \gamma \mathbb{E}_\pi [\mathcal{V}^\pi(s_{t+1})]. \quad (14)$$

Hence, the optimal value function is written as follows:

$$\mathcal{V}^*(s) = \max_a \{ \mathcal{Q}^*(s, a) \}. \quad (15)$$

To solve (15), we can update the Q-function to determine the optimal Q-values of all state-action pairs by using the following rules [25]:

$$\mathcal{Q}_{t+1}(s_t, a_t) = \mathcal{Q}_t(s_t, a_t) + \tau_t \left[ r_t(s_t, a_t) + \gamma \max_{a_{t+1}} \mathcal{Q}_t(s_{t+1}, a_{t+1}) - \mathcal{Q}_t(s_t, a_t) \right], \quad (16)$$

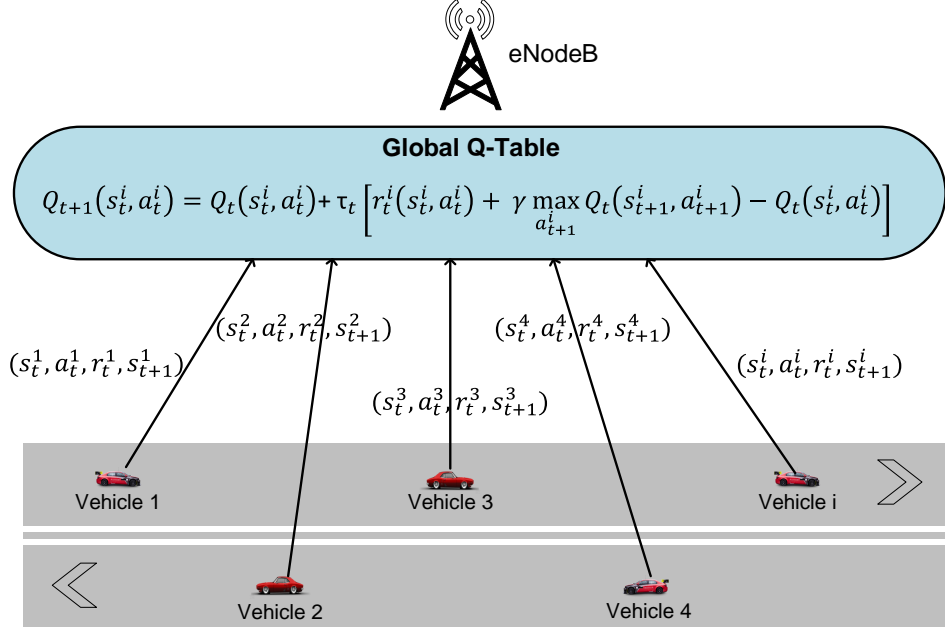


Fig. 2: Parallel Q-learning based model enables simultaneous learning from multiple vehicles.

where  $\tau_t$  denotes the learning rate, determining the impact of new experiences to the current Q-value [25]. By updating the Q-value functions of all state-action pairs by using (16), the algorithm can derive the optimal beam association policy.

### B. Parallel Q-Learning Approach

Note that the conventional Q-learning algorithm can converge to the optimal beam association policy quickly when the system is simple. However, with the dynamics and uncertainties of the system considered in this work, the Q-learning algorithm may take a very long time to obtain the optimal strategy. This is due to the fact that the Q-learning algorithm require a huge number of training episodes to collect enough data for learning. To speed up the Q-learning algorithm, deep reinforcement learning algorithms, e.g., deep double Q-learning, deep Q-learning, and deep dueling [22], [23], are usually adopted in the literature. Nevertheless, these algorithm require high performance computing resources and do not ensure to converge to the optimal policy due to the overestimation of the optimizer [22], [23]. To address these problems, we propose a parallel Q-learning algorithm to quickly obtain the optimal beam association policy by learning from multiple vehicles on the road simultaneously. Thereby, the proposed algorithm can achieve a better

convergence rate compared to the conventional Q-learning algorithm. In other words, the more trials, the better the reward estimates, and thus speeding up the learning process of the algorithm. In particular, vehicles running on the road act as active learners which can help the system simultaneously collect data and significantly speed up the learning process as shown in Fig. 2.

To that end, the parallel Q-learning algorithm employs multiple learning processes. Each learning process is assigned for a vehicle running on the road (in the coverage of the eNodeB). Specifically, each learning process  $i$  updates the Q-value function at the global Q-table as follows:

$$Q_{t+1}(s_t^i, a_t^i) = Q_t(s_t^i, a_t^i) + \tau_t \left[ r_t^i(s_t^i, a_t^i) + \gamma \max_{a_{t+1}^i} Q_t(s_{t+1}^i, a_{t+1}^i) - Q_t(s_t^i, a_t^i) \right], \quad (17)$$

where  $0 \leq \gamma < 1$  is the discount factor that presents the effect of future rewards [25]. In particular, when  $\gamma$  is low, e.g., close to 0, the learning process prefers the current reward. Differently, when  $\gamma$  is high, e.g., close to 1, the long-term reward will be considered. In this work, we set  $\gamma$  the same for all vehicles, i.e., learners.  $r_t^i(s_t^i, a_t^i)$  is the immediate reward when vehicle  $i$  performs action  $a_t^i$  at state  $s_t^i$  (computed using equation 5 above).  $\tau_t$  is the learning rate at decision epoch  $t$  [25]. Note that the learning rate can be fixed at a constant value or it can be adjust when running the algorithm. In this paper, the learning rate is fixed during the training process and is the same for all learning processes. At each decision epoch and given a current state, i.e., RSSI level and current connected beam, the current vehicle chooses to connect to a beam (following the current beam association policy sent from the eNodeB) and observes the data rate of the connected beam as well as the next state. Then, these observations are sent to the eNodeB for learning by the corresponding learning process to update the global Q-table (equation 17). Algorithm 1 describes the fundamental of the proposed parallel Q-learning algorithm.

In particular, vehicle  $i$  first observes the current state  $s_t^i \in \mathcal{S}$  and performs action  $a_t^i$  based on the  $\epsilon$ -greedy policy [32]. Then, the eNodeB selects an action that maximizes the Q-value function with probability  $1 - \epsilon$  and a random action with probability  $\epsilon$ . Then the eNodeB sends this action to vehicle  $i$  to perform. In this work, we gradually reduce the value of  $\epsilon$ . In other words, the algorithm first chooses random actions and gradually change to the deterministic strategy, i.e., choose an action with the highest Q-value at a given state. To that end,  $\epsilon$  is set at a high value (e.g., 1) when the algorithm starts running. Then, at later iterations, the value of  $\epsilon$  is slowly reduced to a small value (e.g., 0.1). After performing action  $a_t^i$ , vehicle  $i$  observes immediate data rate  $r_t^i(s_t^i, a_t^i)$  and next state  $s_{t+1}^i$ . These observations are then sent to the eNodeB

---

**Algorithm 1** Parallel Q-learning Algorithm for Vehicle  $i$ 

---

- 1: **for**  $t=1$  to  $T$  **do**
- 2:     Vehicle  $i$  observes the current state  $s_t^i \in \mathcal{S}$  and execute action  $a_t^i \in \mathcal{A}$  based on the  $\epsilon$ -greedy policy.
- 3:     Vehicle  $i$  observes the immediate reward  $r_t^i$  and new state  $s_{t+1}^i \in \mathcal{S}$ .
- 4:     Vehicle  $i$  sends transition  $(s_t^i, a_t^i, r_t^i, s_{t+1}^i)$  to the eNodeB for learning by updating the table entry of  $Q(s_t^i, a_t^i)$  as follows:

$$Q_{t+1}(s_t^i, a_t^i) = Q_t(s_t^i, a_t^i) + \tau_t \left[ r_t^i(s_t^i, a_t^i) + \gamma \max_{a_{t+1}^i} Q_t(s_{t+1}^i, a_{t+1}^i) - Q_t(s_t^i, a_t^i) \right] \quad (18)$$

- 5:     Replace  $s_t^i \leftarrow s_{t+1}^i$ .

- 6: **end for**
- 

for learning. Note that the learning process of each vehicle is independent from others, and all the learning processes share the same global Q-table. By doing that, the Q-table is updated with more experiences from multiple vehicles running on the road. As such, the convergence rate and convergence time of the parallel Q-learning algorithm will be better than that of the conventional Q-learning algorithm as demonstrated in the simulation results in the following section.

The convergence of our proposed parallel Q-learning algorithm can be guaranteed if its learning processes are serializable [33]. In this case, the parallel Q-learning algorithm can achieve the optimal policy as the one obtained by the Q-learning algorithm. In particular, multiple learning processes (corresponding to multiple vehicles running on the road) simultaneously update different non-related states can be considered as independent processes. As a result, these processes are serialized. Note that as the learning processes update the global Q-table simultaneously, the selection of an action of a learning process may be based on the new Q-value that updated by the other learning process. Specifically, at state  $s$ , a learning process chooses to perform action  $a$  that maximizes the Q-value function. However, another learning process may reach state  $s$  before, make action  $a'$ , and update the Q-value of action  $a'$  to be the highest value. In this case, action  $a$  may still be selected by the  $\epsilon$ -greedy policy mentioned above. In other words, an iteration for exploitation becomes an iteration for exploration. As stated in [25], the algorithm is ensured to converge



to the optimal solution if  $\tau_t$  is nonnegative, deterministic, and follows the following rules:

$$\tau_t \in [0, 1), \sum_{t=1}^{\infty} \tau_t = \infty, \text{ and } \sum_{t=1}^{\infty} (\tau_t)^2 < \infty. \quad (19)$$

Given (19), the convergence of the proposed parallel Q-learning algorithm to the optimal policy is formally stated in Theorem 3 below.

**THEOREM 3.** *Given the learning processes are serializable and under the conditions of  $\tau_t$  in Eq. (19), the parallel Q-learning algorithm is ensured to converge to the optimal policy.*

*Proof:* The proof of Theorem 3 is presented in Appendix C. ■

### C. Impact of High Mobility on Convergence Time

As mentioned, the proposed parallel Q-learning is particularly useful in vehicular networks where multiple vehicles can act as active learners to help the system simultaneously collect data, i.e., experiences. As such, the algorithm can effectively learn and adjust its optimal policy. Moreover, the high mobility of vehicles is also exploited in our proposed parallel learning algorithm. Specifically, when the vehicle's velocity increases, i.e., moving faster on the road, more samples/experiences (over the same period of time) can be collected for the algorithm to learn. The algorithm hence converges to the optimal policy faster. In the simulations below, we can observe that the convergence time (to the optimal association policy) reduces from 800s to 200s when the velocity increases from 2 m/s to 9 m/s.

### D. Complexity and Overhead of Parallel Q-Learning

The proposed parallel Q-learning algorithm is efficient with low computational complexity and memory complexity. As mentioned, the state space of our system includes only the current RSSI level and the current connected beam. For that, the number of states in our system can be defined as  $|A| = M \times K \times N$ . As such, in common mmWave vehicular networks setting with a few mmBSs, the number of state is small, e.g., 180 states in our simulation system in Section V, and thus the size of the global Q-table is also small. Hence, the algorithm can obtain the optimal beam association strategy quickly as the lookup and update table processes are very fast.

Regarding the computational complexity, our proposed algorithm only performs basic calculations without any complex functions as in the other reinforcement learning algorithms, e.g., deep double Q-learning, deep Q-learning, and deep dueling [22], [23]. These algorithms implement deep neural networks to approximate the Q-value function to obtain the optimal policy with complicated mathematical operations, e.g., multiply matrices and gradient descent. As a result, they require longer time to process and higher computing resources compared to our proposed parallel Q-learning algorithm. In addition, in this work, we deploy only one Q-table at the eNodeB to store the Q-values for all state-action pairs instead of implementing a separated Q-tables on each vehicle with limited resources. As a result, the computing complexity is moved to the eNodeB which has sufficient resources to obtain the optimal policy in a short time.

Finally, our proposed parallel Q-learning algorithm incurs minimal communication overhead. In particular, as mentioned in Section III, the state space of the system consists of the current RSSI level and the current connected beam of the vehicle. The RSSI level can be inferred by the mmBS through the signals received from the vehicle. Moreover, the mmBS can always know which beam the vehicle connected to. These information are sent to the eNodeB through the backhaul link with high bandwidth. Furthermore, in intelligent transport systems [35], the location information of vehicles is frequently reported to the RSU, i.e., mmBS. Thus, to update event  $e_s$  of the SMDP, the eNodeB can collect the information of each vehicle through the mmBSs. Therefore, our proposed solution does not add additional overheads to the current ITS standards.

## V. PERFORMANCE EVALUATION

In this section, we investigate the performance of the proposed algorithm in several scenarios. Specifically, we first describe the simulation environment and related parameters. Then, the simulation results are presented.

### A. Parameter Setting

We consider a road with a length of 350 meters in the coverage of an eNodeB. On the considered road, 6 mmBSs are deployed. Each mmBS is equipped with 3 orthogonal beams. Each beam is assumed to cover an area (on the considered road) ranging randomly from 60 meters to 110 meters. The blocking probability

(including both temporary and permanent blockages) of each beam is generated randomly from 0 to 1. We define 10 RSSI levels for each beam corresponding to 10 data rates ranging from 0 to  $R_{\max} = 9$  Gbps, i.e.,  $r_{n,k} \in \{0, 1, \dots, 9\}$ . Unless otherwise stated, at each decision epoch, a vehicle enters the road with probability  $\lambda = 0.5$ . The handover time is set at 0.5 seconds [29], [31].  $z$  is set at 5 meters. The vehicle speed follows the Gaussian distribution. The mean speed of vehicles is then varied from 1 m/s to 9 m/s (about 4 km/h to 32 km/h) in several scenarios to demonstrate the effectiveness of the proposed solution under high mobility. During a decision epoch, the vehicle's speed remains unchanged. It is important to note that the proposed parallel Q-learning algorithm can learn without requiring these parameters in advance. Instead, the algorithm will learn them by interacting with the environment. For the proposed parallel Q-learning and Q-learning algorithms, the discount factor and learning rate are set at 0.1 and 0.0005, respectively. Moreover, for the  $\epsilon$ -greedy method, the initial value of  $\epsilon$  is set at 1 and gradually reduced to 0.1 at the final iterations.

We compare our proposed algorithm with two other methods: (i) *MaxRate* and (ii) *Upper Bound*.

- **MaxRate:** This scheme first explores all available beams at the current location. Then, the beam with the highest RSSI level will be selected to connect. Once *MaxRate* selects the best beam, it will keep connecting to this beam until the end of the current decision epoch. This scheme is used to show the performance of non-adaptive and greedy solutions. As in mmWave systems the temporal degradation of the channel quality frequently occurs, the best beam at the current time may become worse at a later time. Thus, this scheme results in poor system performance in terms of data rate, the number of handovers, and disconnection time.
- **Upper Bound:** This scheme is assumed to know the prior knowledge about the blocking probability of all available beams in the current location. Then, the beam with the lowest blocking probability will be chosen for the vehicle to connect. This scheme is adopted to show the optimistic upper bound of the system performance.

The evaluation metrics are the average data rate, the disconnection time, and the number of handovers. The average data rate is defined as the data received (in bits) by a vehicle running on the road in a second. The number of handovers is defined as the total number of handovers that a vehicle needs to do when running on the road. The disconnection time is defined as the total time that a vehicle cannot communicate with

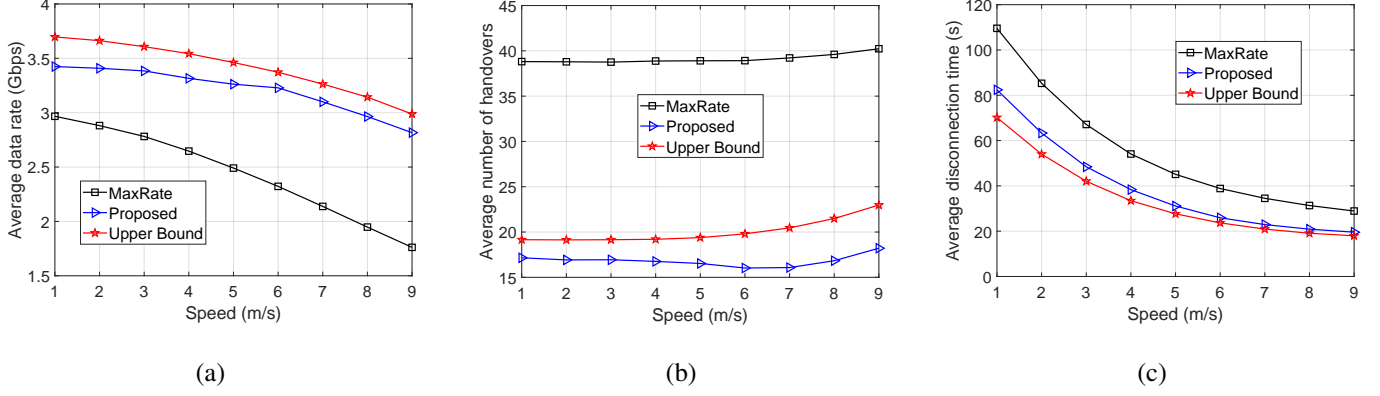


Fig. 3: (a) Average throughput (Gbps), (b) average number of handovers, and (c) average disconnection time vs. average speed of vehicles.

mmBSs. The results of the proposed solution are obtained by running the parallel Q-learning algorithm in 20,000 iterations.

## B. Simulation Results

*a) Performance Evaluation:* We first vary the mean speed of vehicles running on the road and evaluate the performance of the parallel Q-learning algorithm in terms of the average data rate, the disconnection time, and the number of handovers as shown in Fig. 3. Obviously, the average data rate of the vehicle decreases when the mean speed increases as shown in Fig. 3(a). The reason is that the effects of mobility on the handover. In particular, in the case that the vehicle chooses to handover to a new beam and its speed is high, the vehicle may move to another beam before the handover is finished. This results in lower data rates. It is worth noting that by learning the environment parameters, our proposed solution achieves better data rates than that of the *MaxRate* scheme and close to the *Upper Bound* scheme. As can be seen in Fig. 3(b), when the speed increases, our proposed solution chooses to reduce the number of handovers to avoid the negative effect of mobility. In contrast, other solutions with fixed policies cannot learn this information, and thus they do not reduce the number of handovers. It is important to note that, when the speed is higher than 7 m/s (about 25 km/h), the number of handovers increases for all schemes (slightly increase for our proposed solution). This is because at very high speeds, the vehicle moves out the coverage of a beam before finish the handover to connect to this beam, thereby it needs to do the

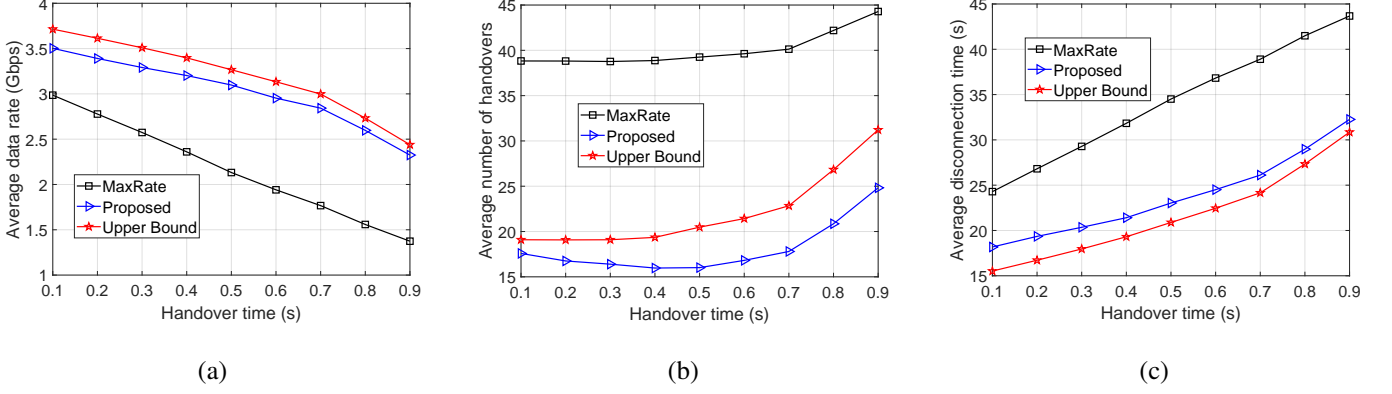


Fig. 4: (a) Average throughput (Gbps), (b) average number of handovers, and (c) average disconnection time vs. average time for handover.

handover again. It is important to note that, at several locations, the only option is to handover to a new beam. Thus, the number of handovers slightly increases for our proposed solution in this case. Finally, as shown in Fig. 3(c), the total disconnect time for all schemes decreases when the vehicle's speed increases. The reason is that with higher speed, the vehicle will spend less time on the road. Note that by using the learning algorithm, our proposed solution achieves lower disconnection time than that of *MaxRate* scheme and close to *Upper Bound* scheme.

Next, we fix the mean speed of vehicles at 7 m/s (about 25 km/h), which is a typical vehicle urban speed [17] and vary the time for the handover to show the average data rate, number of handover, and disconnection time obtained by the proposed parallel Q-learning algorithm as shown in Fig. 4. Clearly, when the time for the handover increases, the disconnection time increases, and thus the average data rates of all solution decrease as shown in Fig. 4(a) and Fig. 4(c). Again, the proposed solution possesses better performance in terms of data rate and disconnection time than those of *MaxRate* scheme and close to that of *Upper Bound* solution. The reason is that our proposed solution can learn and minimize the number of handovers when the time for the handover increases. In particular, as shown in Fig. 4(b), when the time for handover increases from 0.1 seconds to 0.5 seconds, the number of handovers of the proposed solution decreases as our learning algorithm adapts its policy to minimize the number of the handovers and thus maximize the data rate for the vehicle (when the environment parameters are not available in advance).

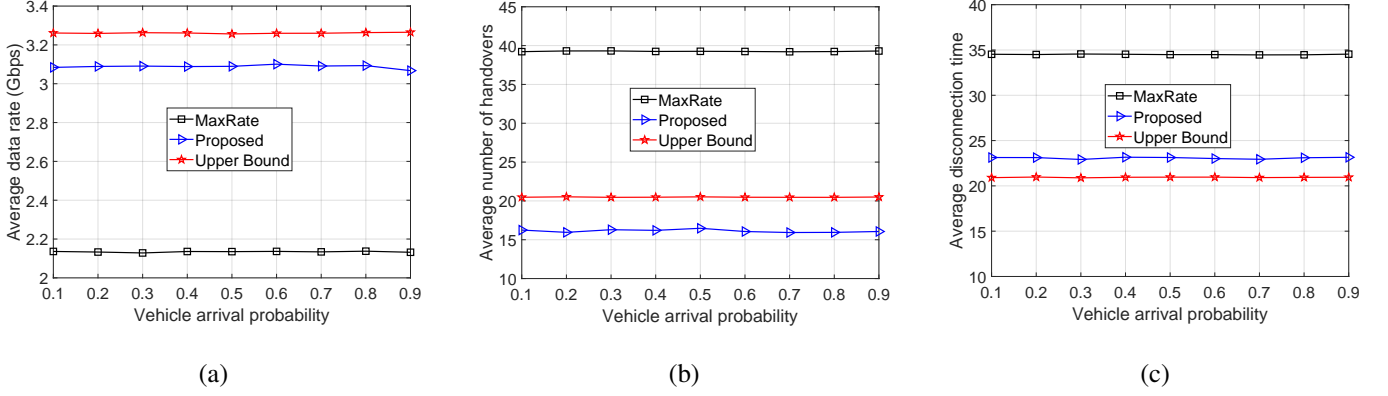


Fig. 5: (a) Average throughput (Gbps), (b) average number of handovers, and (c) average disconnection time vs. vehicle arrival probability.

However, when the time for the handovers is too large (i.e.,  $\geq 0.5$ ) the number of handovers increases. Similar to the previous scenario, when the handover is too long, the vehicle may move out of the target beam, and thus it needs to do the handover again. Nevertheless, by taking the advantage of online learning, our proposed solution has the lowest number of handovers compared to other solutions.

Finally, in Fig. 5, we vary the probability that a vehicle enters the road at each decision epoch to evaluate the performance of the proposed solution. Similar to other scenarios, by learning the environment parameters, i.e., blocking probability, vehicle's speed, and handover time, our proposed solution achieves better performance than that of *MaxRate* scheme in terms of data rate, number of handovers, and disconnection time. Note that our proposed solution's performance is close to that of the optimistic upper bound, i.e., *Upper Bound* scheme.

*b) Convergence:* In Fig. 6, we evaluate the convergence rates of the proposed parallel Q-learning and the Q-learning algorithms. Obviously, the parallel Q-learning algorithm can obtain the optimal beam association policy in less than 1,000 iterations while the Q-learning algorithm needs more than 40,000 iterations. This result confirms the analysis in Section IV-B. Specifically, by learning from multiple vehicles on the road at the same time, the proposed parallel algorithm has more experiences to learn and quickly converge to the optimal policy.

Next, in Fig. 7, we compare the convergence rates of the parallel Q-learning with different numbers of

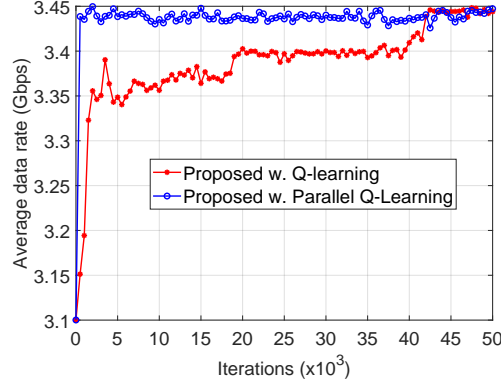


Fig. 6: Convergence rates.

learners, i.e., the number of vehicles. Clearly, the higher number of learners results in better performance. In particular, when the parallel Q-learning runs with only 2 learners, the performance is the worst. When the number of learners increases to 10, the performance of the algorithm is improved. Finally, in the case that we do not limit the number of learners (i.e., learning from all the vehicles running on the road), the algorithm achieves the best performance and quickly convergences to the optimal beam association policy. This implies that by leveraging the fact that there are often numerous vehicles on the road, our proposed parallel Q-learning algorithm can significantly improve the system performance compared to conventional methods.

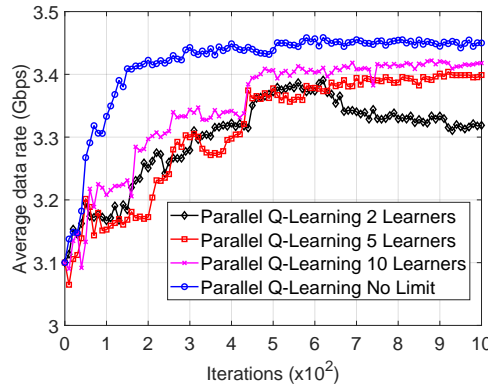


Fig. 7: Convergence rates of the parallel Q-learning with different numbers of learners.

Next, we investigate the convergence time of the proposed parallel Q-learning and the Q-learning

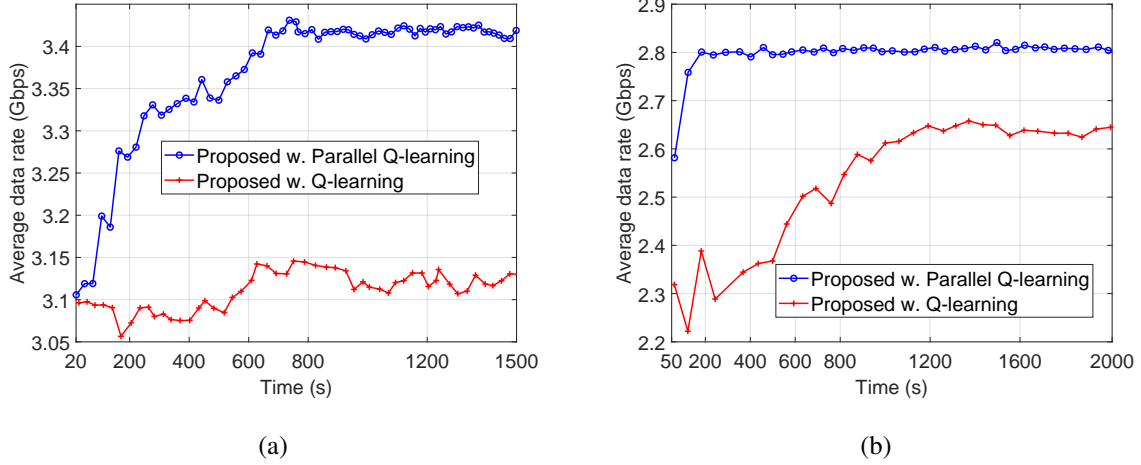


Fig. 8: Convergence time of the algorithms when the average speed of vehicles is (a) 2 m/s and (b) 9 m/s.

algorithms when the average speed of vehicles is low (2 m/s) and high (9 m/s) as shown in Fig. 8(a) and Fig. 8(b), respectively. As discussed in Section IV-C, increasing the speed of vehicles leads to better convergence time of the algorithm as vehicles can collect more experiences for the learning process. As shown in Fig. 8(a), when the speed of vehicles is 2 m/s, the parallel Q-learning algorithm requires at least 600 seconds to obtain the optimal beam association/handover policy. In contrast, when the speed of vehicles is 9 m/s, the algorithm can obtain the optimal association policy within 200 seconds as shown in Fig. 8(b). In all the cases, the Q-learning algorithm still cannot converge to the optimal policy after 2,000 seconds. Note that the average data rate (after obtain the optimal beam association strategy) achieved by the proposed solution in the case the speed of vehicles is 9 m/s lower than that of the case when the speed of vehicles is 2 m/s. As mentioned, this is stemmed from the effects of mobility on the handover. Specifically, in the case that the vehicle chooses to handover to a new beam and its speed is high, the vehicle may move to another beam before the handover is finished. This results in lower data rates.

Finally, in Fig. 9, we compare the convergence rates of the proposed algorithm and the latest advance in deep reinforcement learning, i.e., deep dueling algorithm. In particular, the deep dueling reinforcement learning algorithm implements two flows of hidden layers to separately estimate the advantage and value functions [22], [23]. Recent works demonstrated that the deep dueling algorithm is superior to other deep reinforcement learning algorithms, e.g., deep Q-learning and deep double Q-learning [22], [23]. As shown



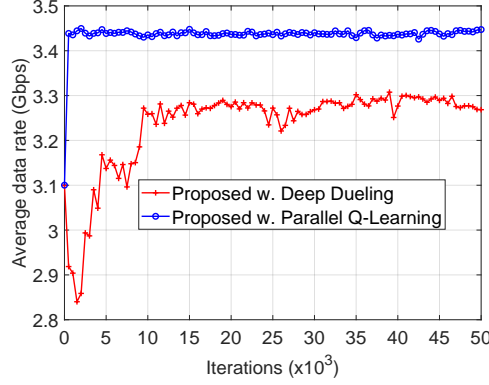


Fig. 9: Convergence rates.

in Fig. 9, our proposed solution can obtain to the optimal beam association strategy in less than 1,000 iterations while the deep dueling cannot converge to the optimal solution after 50,000 iterations. The reason is that our proposed parallel Q-learning algorithm can learn from multiple vehicles running on the road simultaneously. In contrast, the deep dueling algorithm only learn from a single vehicle at a time resulting in poor performance.

## VI. CONCLUSION

In this paper, we have developed an optimal beam association framework for high mobility mmWave vehicular networks, aiming to maximize the system performance in terms of average data rates, number of handovers, and disconnection time of vehicles. The proposed parallel Q-learning algorithm leverages the inherent feature of vehicular networks that there are usually multiple vehicles on the road. By collecting experiences/samples simultaneously from all vehicles, the algorithm converges to the optimal policy much faster than the conventional Q-learning and even its latest deep reinforcement learning framework. Extensive simulations have proved that our proposed parallel Q-learning algorithm can increase the average data rate by 60% and reduce the disconnection time by 33% compared to the conventional solution. In addition, by learning the RSSI profiles of beams and blockages on the road, our proposed solution can achieve the performance close to that of the hypothetical scheme which requires complete environment information in advance. We also observed that the high mobility of the vehicles was actually helpful in speeding up the convergence of the algorithm to the optimal association policy.

## APPENDIX A

### THE PROOF OF LEMMA 1

First, we define a sequence of matrices as  $\{A_n : n \geq 0\}$ . If  $\lim_{n \rightarrow \infty} A_n(s'|s) = (s'|s), \forall (s, s') \in \mathcal{S} \times \mathcal{S}$ , we have  $\lim_{n \rightarrow \infty} A_n = A$ . Now, we define the Cesaro limit (denoted by C-lim) [21] of the sequence as follows:

$$C\text{-}\lim_{N \rightarrow \infty} = \lim_{N \rightarrow \infty} \frac{A_0 + A_1 + \dots + A_n + \dots + A_{N-1}}{N}. \quad (20)$$

Thus,  $A$  is the Cesaro limit (of order one) of  $\{A_n : n \geq 0\}$  if

$$\lim_{N \rightarrow \infty} \frac{1}{N} \sum_{n=0}^{N-1} A_n = A. \quad (21)$$

In a short form, we have:

$$C\text{-}\lim_{N \rightarrow \infty} A_N = A \quad (22)$$

The limiting matrix  $\bar{\mathcal{L}}$  is then formulated as follows:

$$\bar{\mathcal{L}} = C\text{-}\lim_{N \rightarrow \infty} \mathcal{L}^N. \quad (23)$$

Let's denote  $\bar{l}(s'|s)$  as the  $(s'|s)$ -th element of  $\bar{\mathcal{L}}$ . Thus, for each  $s$  and  $s'$ , we have the following:

$$\bar{l}(s'|s) = \lim_{N \rightarrow \infty} \frac{1}{N} \sum_{n=1}^N l^{n-1}(s'|s), \quad (24)$$

where  $l^0(s'|s)$  denotes a element of an  $\mathcal{S} \times \mathcal{S}$  identity matrix, and  $l^{n-1}$  is a component of  $\mathcal{L}^{n-1}$ . Given  $\mathcal{L}$  is aperiodic, we have  $\lim_{N \rightarrow \infty} \mathcal{L}^N$  equals to  $\bar{\mathcal{L}}$ . Thus, the limiting matrix exists.

## APPENDIX B

### THE PROOF OF THEOREM 2

In this proof, we first show that the underlying Markov chain is irreducible. In particular, we will prove that the learning process can move from a given state to any states after a finite number of steps. As mentioned, the system state space  $\mathcal{S}$  is the combination of the RSSI level and the connected beam of the current vehicle. At state  $s = (l, b_{n,k})$ , if the vehicle to connect to beam  $b_{n',k'}$  and the RSSI level when connect to this beam is  $l'$ , the system moves to state  $s' = (l', b_{n',k'})$ . The new RSSI level  $l'$  can be any of levels in  $\mathcal{R}$  as the RSSI level depends on the environmental conditions, e.g., channel conditions, and the blockage probability. In addition, the vehicle can be able to connect to all beams when it is moving

on the road. When the vehicle moves out of the considered road, the system will wait for a new vehicle enters the road and move to a new state. Thus, from a given state  $s$ , the system can move to any other state  $s' \in \mathcal{S}$  after a finite number of steps. In other words, the state space  $\mathcal{S}$  (which is the combination of the RSSI level and the connected beam of the current vehicle) contains only one communicating class, and the underlying Markov chain is irreducible. As such, the long-term average data rate  $\mathcal{R}(\pi)$  does not depend on the initial state and is well defined  $\forall \pi$  [24]. As a result, the algorithm can always converge to the optimal beam association policy regardless of the initial system state  $s_0$ .

## APPENDIX C

### THE PROOF OF THEOREM 3

In this proof, we show that the proposed parallel Q-learning algorithm is ensured to converge to the optimal policy, i.e.,  $\mathcal{Q}_t(s, a) \rightarrow \mathcal{Q}^*(s, a)$  as  $t \rightarrow \infty$ . As mentioned in Section IV-B, the learning processes in our proposed algorithm are serializable. Thus, the convergence proof of the parallel Q-learning is similar to that of the Q-learning algorithm.

The key idea of this proof is using the action-replay process (ARP) (i.e., an artificial controlled Markov decision process) [25]. This action-relay process is defined based on the episode sequence and the learning rate. First, we denote  $\{\langle s, t \rangle\}$  as the state space of the ARP [25]. Here,  $s$  is a state in the actual process,  $t \geq 1$  denotes the ARP's level. In addition, the action space of the ARP is denoted as  $\{a\}$  in which  $a$  is a action in the actual process.

Next, at state  $\langle s, t \rangle$ , if action  $a$  is chosen, the state transition consequence and the stochastic reward of the ARP can be formulated as follows:

$$\mathbf{i}_* = \begin{cases} \operatorname{argmax}_i \{t^i \leq t\}, & \text{if } (s, a) \text{ has been taken before decision epoch } t, \\ 0, & \text{otherwise,} \end{cases} \quad (25)$$

where  $t^i$  represents the  $i^{\text{th}}$  time when performing action  $a$  given state  $s$ . As such,  $t^{i_*}$  is the last time at which action  $a$  is taken at state  $s$  in the real process before decision epoch  $t$ . The reward equals to  $\mathcal{Q}_0(s, a)$  if  $i_* = 0$ . Moreover, in this case, the action-replay process is absorbed. Otherwise, we denotes the index

of the decision epoch which is taken from the existing samples from the real process as follows:

$$\mathbf{i}_e = \begin{cases} i_*, & \text{with probability } \tau_{t^{i_*}}, \\ i_* - 1, & \text{with probability } (1 - \tau_{t^{i_*}})\tau_{t^{i_*}-1}, \\ i_* - 2, & \text{with probability } (1 - \tau_{t^{i_*}})(1 - \tau_{t^{i_*}-1})\tau_{t^{i_*}-2}, \\ \vdots & \\ 0, & \text{with probability } \prod_{i=1}^{i_*}(1 - \tau_{t^i}), \end{cases} \quad (26)$$

Similar as above, when  $i_e = 0$ , the reward is  $\mathcal{Q}_0(s, a)$  and the process is absorbed. Otherwise, taking  $i_e \neq 0$  results reward  $r_{t^{i_e}}$  and a state transition to  $\langle s'_{t^{i_e}}, t^{i_e} - 1 \rangle$ .

Putting the above and Lemma B in [25] together, we have  $\mathcal{Q}_t(s, a) \rightarrow \mathcal{Q}_{ARP}^*(\langle s, t \rangle, a)$ ,  $\forall a, s$ , and  $t \geq 0$ , in which  $\mathcal{Q}_t(s, a)$  is the optimal action values of the ARP with state  $\langle s, t \rangle$  and action  $a$  [25, Lemma A]. Let's denote  $r^*$  as the bound of the reward, and thus  $r^* \geq |r_t|, \forall t$ . With loss of generality, assuming that  $\mathcal{Q}_t(s, a) < \frac{r^*}{(1-\gamma)}$  with  $r^* \geq 1$  [25]. Thus, with  $\chi > 0$ , we can find  $\xi$  so that

$$\gamma^\xi \frac{r^*}{1-\gamma} < \frac{\chi}{6}. \quad (27)$$

By using Lemma B.4 in [25], the comparison of between the value of performing  $a_1, \dots, a_\xi$  in the real process, i.e.,  $\bar{\mathcal{Q}}(s, a_1, \dots, a_\xi)$ , with that of taking these actions in the ARP, i.e.,  $\bar{\mathcal{Q}}_{ARP}(\langle s, t \rangle, a_1, \dots, a_\xi)$ , is formulated as follows:

$$\begin{aligned} & |\bar{\mathcal{Q}}_{ARP}(\langle s, t \rangle, a_1, \dots, a_\xi) - \bar{\mathcal{Q}}(s, a_1, \dots, a_\xi)| < \\ & \frac{\chi(1-\gamma)}{6\xi r^*} \frac{2\xi r^*}{1-\gamma} + \frac{2\chi}{3\xi(\xi+1)} \frac{\xi(\xi+1)}{2} = \frac{2\chi}{3}. \end{aligned} \quad (28)$$

Based on Lemma B.4 in [25], we can say that taking only  $\xi$  actions results in a small different of less than  $\frac{\chi}{6}$  for both the real process and the action-replay process. In addition, we can apply (28) to an set of actions in both the action-replay and the real processes. As such,  $|\mathcal{Q}_{ARP}^*(\langle s, t \rangle, a) - \mathcal{Q}^*(s, a)| < \chi$ . Thus,  $\mathcal{Q}_t(s, a) \rightarrow \mathcal{Q}^*(s, a)$  when  $t \rightarrow \infty$  with probability 1.

## REFERENCES

- [1] V. Va, T. Shimizu, G. Bansal, and R. W. Heath Jr, "Millimeter wave vehicular communications: A survey," *Foundations and Trends in Networking*, vol. 10, no. 1, pp. 1-113, Jun. 2016.
- [2] D. Yan, H. Yi, D. He, K. Guan, B. Ai, Z. Zhong, J. Kim, and H. Chung, "Channel Characterization for Satellite Link and Terrestrial Link of Vehicular Communication in the mmWave Band," *IEEE Access*, vol. 7, pp. 173559-173570, Nov. 2019.

- [3] A. D. Angelica, "Google's self-driving car gathers nearly 1 GB/sec", [Online]. Available: <http://www.kurzweilai.net/googles-self-driving-cargathers-nearly-1-gbsec>.
- [4] X. Wang, L. Kong, F. Kong, F. Qiu, M. Xia, S. Arnon, and G. Chen, "Millimeter wave communication: A comprehensive survey," *IEEE Communications Surveys & Tutorials*, vol. 20, no. 3, pp. 1616-1653, Jun. 2018.
- [5] O. Semiari, W. Saad, and M. Bennis, "Joint millimeter wave and microwave resources allocation in cellular networks with dual-mode base stations," *IEEE Transactions on Wireless Communications*, vol. 16, no. 7, pp. 4802-4816, Jul. 2017.
- [6] M. Polese, M. Giordani, M. Mezzavilla, S. Rangan, and M. Zorzi, "Improved handover through dual connectivity in 5G mmWave mobile networks," *IEEE Journal on Selected Areas in Communications*, vol. 35, no. 9, pp. 2069-2084, Sept. 2017.
- [7] M. Feng, and S. Mao, "Dealing with Limited Backhaul Capacity in Millimeter-Wave Systems: A Deep Reinforcement Learning Approach," *IEEE Communications Magazine*, vol. 57, no. 3, pp. 50-55, Mar. 2019.
- [8] C. Fan, B. Li, C. Zhao, W. Guo, and Y.-C. Liang, "Learning-based spectrum sharing and spatial reuse in mm-wave ultradense networks," *IEEE Transactions on Vehicular Technology*, vol. 67, no. 6, pp. 4954-4968, Jun. 2018.
- [9] R. Amiri and H. Mehrpouyan, "Self-organizing mm wave networks: a power allocation scheme based on machine learning," *Global Symposium on Millimeter Waves (GSMM)*, Boulder, CO, USA, 22-24 May 2018.
- [10] J. Qiao, X. S. Shen, J. W. Mark, and L. Lei, "Video quality provisioning for millimeter wave 5G cellular networks with link outage," *IEEE Transactions on Wireless Communications*, vol. 14, no. 10, pp. 5692-5703, Oct. 2015.
- [11] S. Zang, W. Bao, P. L. Yeoh, B. Vucetic, and Y. Li, "Managing Vertical Handovers in Millimeter Wave Heterogeneous Networks," *IEEE Transactions on Communications*, vol. 67, no. 2, pp. 1629-1644, Feb. 2019.
- [12] F. Sotrohi and W. Yu, "Hybrid analog and digital beamforming for mmWave OFDM large-scale antenna arrays," *IEEE Journal on Selected Areas in Communications*, vol. 35, no. 7, pp. 1432-1443, Jul. 2017.
- [13] N. Garcia, H. Wymeersch, E. G. Strom, and D. Slock, "Location-aided mm-wave channel estimation for vehicular communication," *IEEE 17th International Workshop on Signal Processing Advances in Wireless Communications (SPAWC)*, Edinburgh, UK, Jul. 2016.
- [14] V. Va, T. Shimizu, G. Bansal, and R. W. Heath, "Beam design for beam switching based millimeter wave vehicle-to-infrastructure communications," *IEEE International Conference on Communications (ICC)*, Kuala Lumpur, Malaysia, Jul. 2016.
- [15] Y. Wang, K. Venugopal, A. F. Molisch, and R. W. Heath, "MmWave vehicle-to-infrastructure communication: Analysis of urban microcellular networks," *IEEE Transactions on Vehicular Technology*, vol. 67, no. 8, pp. 7086-7100, Aug. 2018.
- [16] G. H. Sim, S. Klos, A. Asadi, A. Klein, and M. Hollick, "An online context-aware machine learning algorithm for 5G mmWave vehicular communications," *IEEE/ACM Transactions on Networking*, vol. 26, no. 6, pp. 2487-2500, Dec. 2018.
- [17] H. Khan, A. Elgabri, S. Samarakoon, M. Bennis, and C. S. Hong, "Reinforcement Learning Based Vehicle-cell Association Algorithm for Highly Mobile Millimeter Wave Communication," *IEEE Transactions on Cognitive Communications and Networking*, Early Access, 2019.
- [18] M. Giordani, M. Mezzavilla, S. Rangan, and M. Zorzi, "Multi-connectivity in 5G mmWave cellular networks," in *Proc. IFIP Med-Hoc-Net*, Jun. 2016, pp. 17.
- [19] H. Shokri-Ghadikolaei et al., "The impact of beamforming and coordination on spectrum pooling in mmWave cellular networks," in *Proc. ASILOMAR*, Nov. 2016, pp. 2126.
- [20] H. Shokri-Ghadikolaei, F. Boccardi, C. Fischione, G. Fodor, and M. Zorzi, "Spectrum sharing in mmWave cellular networks via cell association, coordination, and beamforming," *IEEE Journal on Selected Areas in Communications*, vol. 34, no. 11, pp. 2902-2917, Nov.

2016.

- [21] M. Puterman, *Markov Decision Processes: Discrete Stochastic Dynamic Programming*, Hoboken, NJ: Wiley, 1994.
- [22] N. V. Huynh, D. T. Hoang, D. N. Nguyen, and E. Dutkiewicz, "Optimal and fast real-time resource slicing with deep dueling neural networks", *IEEE Journal on Selected Areas in Communications*, vol. 37, no. 6, pp. 1455-1470, Jun. 2019.
- [23] N. V. Huynh, D. N. Nguyen, D. T. Hoang, and E. Dutkiewicz, "Jam Me If You Can: Defeating Jammer with Deep Dueling Neural Network Architecture and Ambient Backscattering Augmented Communications", *IEEE Journal on Selected Areas in Communications*, vol. 37, no. 11, pp. 2603-2620, Nov. 2019.
- [24] J. Filar and K. Vrieze, *Competitive Markov Decision Processes*. Springer Press, 1997.
- [25] C. J. C. H. Watkins and P. Dayan, "Q-learning," *Mach. Learn.*, vol. 8, no. 34, pp. 279-292, 1992.
- [26] E. S. Navarro, Y. Lin, and V. Wong, "An MDP-based vertical handoff decision algorithm for heterogeneous wireless networks," *IEEE Transactions on Vehicular Technology*, vol. 57, no. 2, pp. 1243-1254, Mar. 2008.
- [27] M. Mezzavilla, S. Goyal, S. Panwar, S. Rangan, and M. Zorzi, "An MDP model for optimal handover decisions in mmWave cellular networks," in *Proc. EUCNC 2016*, Athens, Greece, Jun. 2016, pp. 100-105.
- [28] H. Elshaer, M. N. Kulkarni, F. Boccardi, J. G. Andrews, and M. Dohler, "Downlink and uplink cell association with traditional macrocells and millimeter wave small cells," *IEEE Transactions on Wireless Communications*, vol. 15, no. 9, pp. 6244-6258, Sep. 2016.
- [29] S. Zang, W. Bao, P. L. Yeoh, B. Vucetic, and Y. Li, "Managing Vertical Handovers in Millimeter Wave Heterogeneous Networks," *IEEE Transactions on Communications*, vol. 67, no. 2, pp. 1629-1644, Feb. 2019.
- [30] Y. Sun, G. Feng, S. Qin, Y.-C. Liang, and T.-S. P. Yum, "The smart handoff policy for millimeter wave heterogeneous cellular networks," *IEEE Transactions on Mobile Computing*, vol. 17, no. 6, pp. 1456-1468, Jun. 2018.
- [31] H. S. Park, Y. Lee, T. J. Kim, B. C. Kim, and J. Y. Lee, "Handover mechanism in NR for ultra-reliable low-latency communications," *IEEE Network*, vol. 32, no. 2, pp. 41-47, Mar. 2018.
- [32] R. S. Sutton and A. G. Barto, *Reinforcement Learning: An Introduction*. Cambridge, MA, USA: MIT Press, 1998.
- [33] M. Camelo, J. Famaey, and S. Latre, "A scalable parallel Q-learning algorithm for resource constrained decentralized computing environments," *Proc. Workshop on Machine Learning in HPC Environments (MLHPC)*, Salt Lake City, UT, USA, Nov. 2016, pp. 27-35.
- [34] F. Jameel, S. Wyne, S. J. Nawaz, and Z. Chang, "Propagation channels for mmWave vehicular communications: State-of-the-art and future research directions," *IEEE Wireless Communications*, vol. 26, no. 1, pp. 144-150, Feb. 2019.
- [35] ETSI TR 102 638 V1.1.1 Intelligent Transport Systems (ITS); Vehicular Communications; Basic Set of Applications; Definitions.
- [36] Q. Li, L. Zhao, J. Gao, H. Liang, L. Zhao, and X. Tang, "SMDP-based coordinated virtual machine allocations in cloud-fog computing systems," *IEEE Internet of Things Journal*, vol. 5, no. 3, pp. 1977-1988, Jun. 2018.
- [37] Y. Koda, K. Yamamoto, T. Nishio, and M. Morikura, "Reinforcement learning based predictive handover for pedestrian-aware mmWave networks," *IEEE Conference on Computer Communications Workshops*, Honolulu, HI, USA, 15-19 Apr. 2018.
- [38] R. Wang, O. Onireti, L. Zhang, M. A. Imran, G. Ren, J. Qiu, and T. Tian, "Reinforcement Learning Method for Beam Management in Millimeter-Wave Networks," *UK/China Emerging Technologies (UCET)*, Glasgow, United Kingdom, 21-22 Aug. 2019.
- [39] Y.-J. Chen, W.-Y. Cheng, and L.-C. Wang, "Learning-assisted beam search for indoor mmwave networks," *IEEE Wireless Communications and Networking Conference Workshops (WCNCW)*, Barcelona, Spain, 15-18 Apr. 2018.